ISSN 1070-3284, Russian Journal of Coordination Chemistry, 2014, Vol. 40, No. 3, pp. 154–159. © Pleiades Publishing, Ltd., 2014.

Crystal Structures and Electrochemical Properties of Two Mn(II) 2-Sulfoterephthalate Complexes with N-Donor Ligands[1]

Y. Ren*, T. Hao, M. Zhang, D. Wang, H. Yu, and Y. Wang

College of Chemistry and Chemical Engineering, Shaanxi Key Laboratory of Chemical Reaction Engineering, Yan'an University, Yan'an, 716000 P. R. China

**e-mail: renyixia1@163.com*

Received November 27, 2012

Abstract—Two Mn(II) sulfoterephthalate complexes, [Mn(HStp)(*o*-Phen)$_2$] (**I**) and [Mn(HStp)(2,2'-Bipy)$_2$] (**II**) (H_3Stp = 2-sulfoterephthalic acid, *o*-Phen = 1,10-phenanthroline, 2,2'-Bipy = 2,2'-bipyridine), were synthesized under hydrothermal condition. Single crystal X-ray diffraction analyses reveal that complexes **I** and **II** possess similar structure, in which the center Mn^{2+} ions are hexa-coordinated with one $Hstp^-$ anion and two N-donor ligands. For both of them, the formation of 3D supramolecular structures are based on both H-bonds and π···π/C–H···π stacking interactions. Electrochemical properties of complexes **I** and **II** have been investigated by means of cyclic voltmetry, which shows that electron transfer between Mn(III) and Mn(II) in electrolysis is quasi-reversible process.

DOI: 10.1134/S1070328414030075

INTRODUCTION

Transitional metal organic complexes have been investigated and developed increasingly in recent years for their diversified structures and potential applications [1–4]. The metal-carboxylate complexes become one of the most important series of metal organic complexes, because of the versatile coordination modes of carboxyl group and the multiform functional properties of these complexes [5–8]. Coordination fashions of the carboxyl group may be mon-dentate, bidentate, bridge, chelate, and multidentate, in result that 0D to 3D metal organic complexes exhibiting kinds of luminescent, electric and magnetic properties [9–11]. The selection of organic ligand could affect the formation and properties of metal organic complexes. 2-Sulfoterephthalate is a rigid and multidentate ligand with seven coordination sites benefited from its two carboxyl groups and one sulfonate group. Its three protons, not all dissociated, could form H-bonds with the adjacent ligands or solvent molecules, and its phenyl ring possibly assembles with some pyridine-containing ligands via π···π stacking, finally constructing high dimensional supramolecule. To our knowledge, the investigations on 2-sulfoterephthalic acid are mainly focused on the *d*- and *f*-block transitional metal complexes (Zn(II), Cd(II), Mn(II), Cu(II), Eu(III), Tb(III)) [12–16], in which only one example reported about manganese(II) complex [14]. A great opportunity to study the structural characterization about the Mn(II) complexes with the 2-$HStp^{2-}$ ligand inspires us to explore the supramolecular complexes from them. Moreover, we introduce two N-donor ligands, 1,10-phenanthroline (*o*-Phen) and 2,2'-bipyridine (2,2'-Bipy) to form H-bonds or π···π stacking interactions and alter the dimension of the supramolecular structure. In this paper, we obtained two Mn(II) supramolecular complexes based on 2-sulfoterephthalate and three N-donor ligands.

[1] The article is published in the original.

EXPERIMENTAL

Materials and methods. All chemicals were commercially available and used as received without further purification. Elemental analyses (CHN) were performed using an Vario EL elemental analyzer. FT-IR spectra were recorded from KBr pellets in the range of 4000–400 cm^{-1} on a Nicolet Avatar 360 FT-IR spectrometer.

Synthesis of [Mn(HStp)(*o*-Phen)$_2$] (I). A mixture of NaH_2Stp (0.013 g, 0.05 mmol), *o*-Phen (0.019 g, 0.1 mmol) and $Mn(OAc)_2 \cdot 4H_2O$ (0.013 g, 0.05 mmol) in 5 mL H_2O was stirred for 15 min, then placed in a 23-mL Teflon-lined autoclave and heated at 140°C for 96 h. The autoclave was cooled over a period of 10 h by natural cooling. The yellow block crystals of **I** were

collected by filtration, washed with ethanol, and dried in air (the yieldwas 12 mg, ~36% based on Mn).

For $C_{32}H_{20}N_4O_7SMn$

anal. calcd., %:	C, 58.28;	H, 3.06;	N, 8.50.
Found, %:	C, 58.47;	H, 3.10;	N, 8.65.

IR (KBr; ν, cm^{-1}): 3450 m, 3072 w, 1713 m, 1625 m, 1517 s, 1427 s, 1270 s, 1225 m, 1176 s, 1071 s, 1018 m, 797 s.

Synthesis of [Mn(HStp)(2,2'-Bipy)$_2$] (II). A mixture of NaH_2Stp (0.013 g, 0.05 mmol), 2,2'-Bipy (0.016 g, 0.1 mmol) and $Mn(OAc)_2 \cdot 4H_2O$ (0.013 g, 0.05 mmol) in 5 mL H_2O was stirred for 15 min, then placed in a 23-mL Teflon-lined autoclave and heated at 140°C for 96 h. The autoclave was cooled over a period of 10 h by natural cooling. The yellow block crystals of **II** were collected by filtration, washed with ethanol, and dried in air (the yield was 19 mg, ~62% based on Mn).

For $C_{28}H_{20}N_4O_7SMn$

anal. calcd., %:	C, 54.99;	H, 3.30;	N, 9.16.
Found, %:	C, 54.62;	H, 3.49;	N, 9.29.

IR (KBr; ν, cm^{-1}): 3450 m, 3071 w, 1712 m, 1597 m, 1520 s, 1408 s, 1267 s, 1240 s, 1171 s, 1068 m, 1016 s, 807 m.

X-ray structure determination. Single crystal X-ray diffraction analyses of the four complexes were carried out on a Bruker SMART APEX CCD diffractometer equipped with a graphite monochromated MoK_α radiation (λ = 0.71073 Å). Raw data were integrated with the SAINT program [17]. The structures were solved by direct methods with SHELXS-97 and refined by full-matrix least-squares on F^2 using SHELXS-97 [18]. An empirical absorption correction was applied with the program SADABS [19]. All non-hydrogen atoms were refined anisotropically. The hydrogen atoms were set in calculated positions and refined by a riding mode. The crystallographic details of complexes **I**, **II** are provided in Table 1, while the selected bond distances and angles of **I**, **II** are listed in Table 2, respectively. All the H-bonds parameters in **I**, **II** are listed in Table 3. Supplementary material for structures **I**, **II** has been deposited with the Cambridge Crystallographic Data Centre (nos. 819170 (**I**), 819171 (**II**); deposit@ccdc.cam.ac.uk or http://www.ccdc.cam.ac.uk).

RESULTS AND DISCUSSION

Single-crystal X-ray diffraction analysis reveals that the asymmetric unit of **I** consists of one Mn^{2+} ion, one $HStp^{2-}$ anion and two *o*-Phen ligands. The central

Table 1. Crystallographic data and structure refinement for complexes **I** and **II**

Parameter	Value	
	I	**II**
Mw	659.52	611.48
T, K	296(2)	296(2)
Crystal system	Triclinic	Triclinic
Space group	$P\bar{1}$	$P\bar{1}$
a, Å	9.5174(6)	9.1988(7)
b, Å	9.7202(6)	9.7582(7)
c, Å	16.8964(11)	16.3634(11)
α, deg	73.3010(10)	101.0390(10)
β, deg	97.6080(10)	98.7040(10)
γ, deg	70.1600(10)	90.9490(10)
V, Å^3	1402.63(15)	1423.49(18)
Z	2	2
ρ_{calcd}, g cm^{-1}	1.562	1.427
μ, mm^{-1}	0.604	0.589
θ Range, deg	2.28–25.25	2.13–25.25
Reflection collected	7080	5091
Unique reflection	5018	5091
R_{int}	0.0181	0
GOOF	1.040	1.037
R_1 ($I > 2\sigma(I)$)	0.0374	0.0401
wR_2 (all data)	0.0913	0.1077
$\Delta\rho_{max}/\Delta\rho_{min}$, *e* Å^{-3}	0.426 and −0.328	0.246 and −0.243

Table 2. Selected bond lengths (Å) and angles (deg) for complexes **I** and **II**

Bond	*d*, Å	Bond	*d*, Å
I		**II**	
Mn(1)–O(1)	2.0816(16)	Mn(1)–O(1)	2.0753(17)
Mn(1)–O(5)	2.1921(16)	Mn(1)–O(5)	2.1871(18)
Mn(1)–N(1)	2.255(2)	Mn(1)–N(1)	2.247(2)
Mn(1)–N(2)	2.260(2)	Mn(1)–N(4)	2.249(2)
Mn(1)–N(4)	2.290(2)	Mn(1)–N(3)	2.259(2)
Mn(1)–N(3)	2.3356(19)	Mn(1)–N(2)	2.280(2)
Angle	ω, deg	Angle	ω, deg
I		**II**	
O(1)Mn(1)O(5)	87.56(6)	O(1)Mn(1)O(5)	91.34(7)
O(1)Mn(1)N(1)	159.28(7)	O(1)Mn(1)N(1)	93.33(7)
O(5)Mn(1)N(1)	83.24(7)	O(5)Mn(1)N(1)	93.33(7)
N(2)Mn(1)N(3)	85.27(7)	O(1)Mn(1)N(4)	93.07(7)
O(1)Mn(1)N(2)	94.34(7)	O(5)Mn(1)N(4)	101.52(8)
O(5)Mn(1)N(2)	117.12(7)	N(1)Mn(1)N(4)	163.68(8)
N(1)Mn(1)N(2)	73.71(7)	O(1)Mn(1)N(3)	164.88(7)
O(1)Mn(1)N(4)	95.01(7)	O(5)Mn(1)N(3)	86.62(7)
N(4)Mn(1)N(3)	71.89(7)	N(1)Mn(1)N(3)	101.74(8)
O(5)Mn(1)N(4)	84.71(7)	N(4)Mn(1)N(3)	72.73(8)
N(1)Mn(1)N(4)	102.54(7)	O(1)Mn(1)N(2)	94.61(7)
N(2)Mn(1)N(4)	156.59(7)	O(5)Mn(1)N(2)	164.93(8)
O(1)Mn(1)N(3)	101.15(7)	N(1)Mn(1)N(2)	72.54(7)
O(5)Mn(1)N(3)	155.54(7)	N(4)Mn(1)N(2)	91.99(7)
N(1)Mn(1)N(3)	94.77(7)	N(3)Mn(1)N(2)	91.11(8)

Table 3. Geometric parametes of hydrogen bonds in **I** and **II***

D–H···A	Distance, Å			Angle DHA, deg
	D–H	H···A	D···A	
I				
O(4)–H(4)···O(2*A*)[a]	0.82	1.72	2.5213(3)	164
II				
O(4)–H(4)···O(2*A*)[b]	0.82	1.81	2.6110(2)	166

* Symmetry codes: [a] $-1+x, y, z$; [b] $x, -1+y, z$.

Mn^{2+} ion is hexa-coordinated with two O atom (O(1) and O(5)) from the carboxylate and the sulfonate groups of one $HStp^{2-}$ anion, four N atoms (N(1), N(2), N(3), and N(4)) from two *o*-Phen ligands, forming a distorted octahedron (Fig. 1a). The range of Mn–N bond lengths is from 2.255 to 2.336 Å and the Mn–O bond lengths are 2.082 and 2.192 Å, which are in the normal scope of Mn–O and Mn–N bonds lengths in reported complexes [20–22].

The uncoordinated O atom of 1-site carboxylate group of one $HStp^{2-}$ anion links the protonated O atoms of 4-site carboxylate group of adjacent $HStp^{2-}$ anion via its hydrogen atom forming H-bond (O(4)–H(4)···O(2*A*); O···O 2.521 Å). As shown in Fig. 2, the H-bonds connect mononuclear Mn molecules into 1D supramolecular chain structure along *x* axis.

For each Mn^{2+} ion, a dihedral angle of 82.6° separates two *o*-Phen ligands, which benefits the formation of π···π stacking interactions in different directions. Actually, the 1D supramolecular chains extend along *x* and *z* axis into 2D supramolecular layer though the face-to-face π···π stacking interactions between *o*-Phen ligands standing out from two angles (Fig. 3). For the face-to-face π···π stacking interactions along *x* axis based on Phen(1) (C(13)–C(24) and N(3)–N(4)), the perpendicular distance is 3.484 Å (Cg–Cg 3.722 Å) (Fig. 4a), while those along *z* axis based on Phen(2) (C(1)–C(12) and N(1)–N(2)) have the perpendicular distance of 3.649 Å (Cg–Cg 4.075 Å) (Fig. 4b). Obviously, the interaction of the former is stronger than that of the later. Furthermore, the 2D supramolecular layers extend along *y* axis into 3D supramolecular structure via the edge-to-face C–H···π stacking interactions between C(27)–H(27) of one $HStp^{2-}$ anion and the Phen(1) ligand (H(27)···Cg(1) 2.856 Å) (Fig. 4c).

The structure of **II** is similar to that of **I** for the similarity of the configuration and the coordination mode of the N-containing ligands. As shown in Fig. 1b, the Mn(II) center is in a hexa-coordinated octahedron configuration by O(1) and O(5) atoms from one $HStp^{2-}$ ligand, N(1) to N(4) atoms from two 2,2'-Bipy ligands. The bond lengths of Mn–N range from 2.247 to 2.280 Å, which are slightly longer than those in **I**. While the bond lengths of Mn–O are 2.075 and 2.187 Å, shorter than those in **I**.

Also complex **II** is firstly constructed from a 1D supramolecular chain based on H-bonds (O(4)–H(4)···O(2*A*); O···O 2.611 Å) between two O atoms from two adjacent $HStp^{2-}$ ligands along *y* axis (Fig. 5). The distance of H-bonds are longer than those in **I**. In **II**, 2D supramolecular layer in *xy* plane are assembled from 1D supramolecular chains via the face-to-face π···π stacking between two adjacent 2,2'-Bipy(1) (N(3), N(4), C(11)–C(20)) ligands (Fig. 6). A dihedral angle of 91.2° is between two 2,2'-Bipy ligands coor-

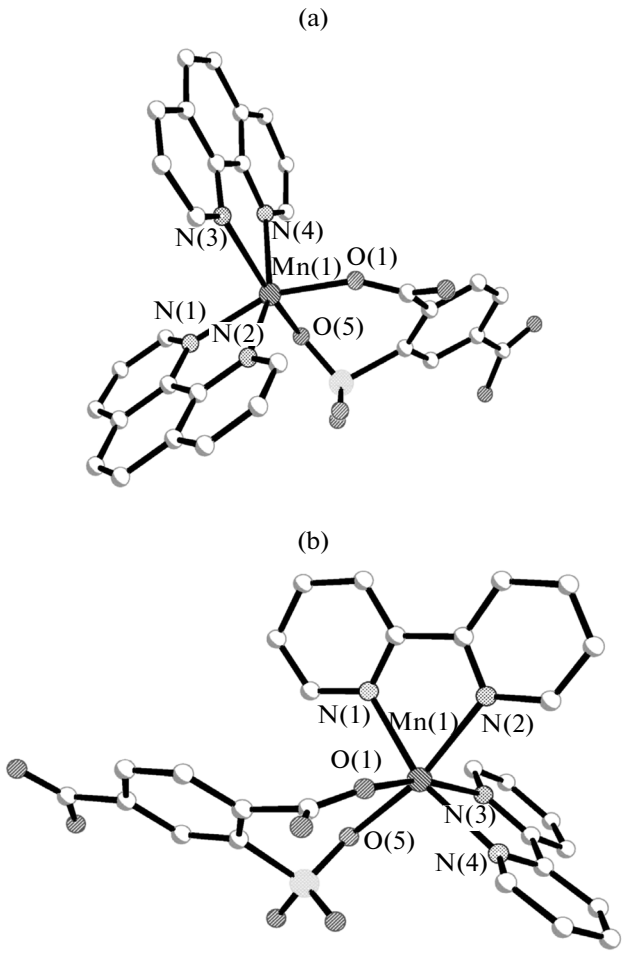

Fig. 1. The coordination environment of Mn^{2+} ion in **I** (a) and **II** (b).

dinated to one Mn^{2+} ion. Then, the edge-to-face C–H···π stacking interactions exist between C(13)–H(13) of 2,2'-Bipy(1) and an adjacent 2,2'-Bipy(2) (3.566 Å) and C(23)–H(23) of one $HStp^{2-}$ ligand and an adjacent 2,2'-Bipy(2) (3.538 Å). These interactions further lead to 3D supramolecular structure from the 2D supramolecular one.

The solid of complexes **I** and **II** are stable at room temperature. IR data show that the absorption bonds resulting from the γ(=C–H) of 1,2,4-substituded phenyl rings at 1071, 797 and 1068, 807 cm^{-1}, and the ν(–C–H) stretching vibrations appear in them at 3072 and 3071 cm^{-1} for **I** and **II**, respectively. The bonds at 1176, 1018 (**I**) and 1171, 1016 cm^{-1} (**II**) indicate the ν_{as} and ν_s vibrations of sulfonate groups of $HStp^{2-}$ ligand in them. The peaks at 1517, 1427 and 1520, 1408 cm^{-1} could be assigned to the asymmetric and symmetric stretching vibrations of carboxyl groups. The middle peaks at 3450 cm^{-1} for them can be attributed to ν(–O–H) stretching vibrations of protonated carboxyl group of $HStp^{2-}$ ligand. The analysis of IR spectrum of them are in agreement with their crystal structures and charge balance consideration.

The thermogravimetric experiments were performed on complexes **I** and **II** in air from 30 to 1000°C. TG curves show both **I** and **II** are one step of weight loss. Complex **I** is stable up to near 300°C, then following the break of the supramolecular framework till 926°C. While for **II**, it begins decomposing from 233°C and the structure collapses up to 840°C. From the results, we can see that two complexes possess high thermal stabilities due to the existence of a great deal of intermolecular interactions, and complex **I** is more stable than **II** due to its stronger H-bonds (the distance of 2.521 Å is less than that of 2.611 Å in complex **II**).

The UV-vis absorption spectra for free ligand and complexes **I** and **II** were recorded in reflectance mode in DMF solution. According to the spectra, the wavelength absorption bands of **I** occur at 268 and 297 nm for free ligand, 270 nm for **I** and 299 nm for **II**, which could be attributed to the π–π* transition of ligand. The absorption band of **I** is much narrower than those of ligand and complex **II**, which may be related to the fact that the π stacking interactions in **I** is weaker than those of **II** [23, 24] (the distance of π stacking interactions in **I** are bigger than those of **II**).

Cyclic voltmmetry was used to investigate the electrochemical properties of complexes **I** and **II** in dry

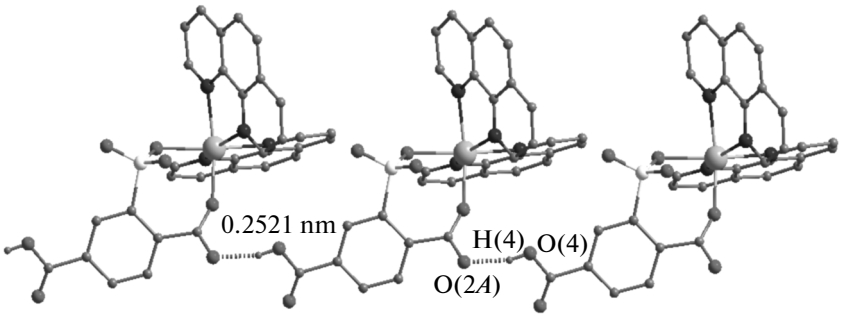

Fig. 2. 1D chain supramolecular structure: along *x* axis in **I**.

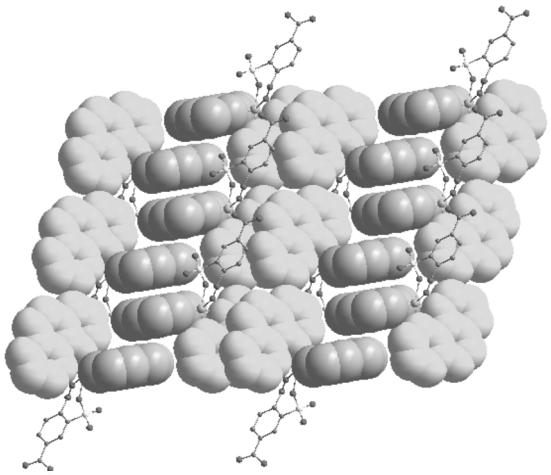

Fig. 3. 2D supramolecule based on π···π stacking interactions in *xz* plane of **I**.

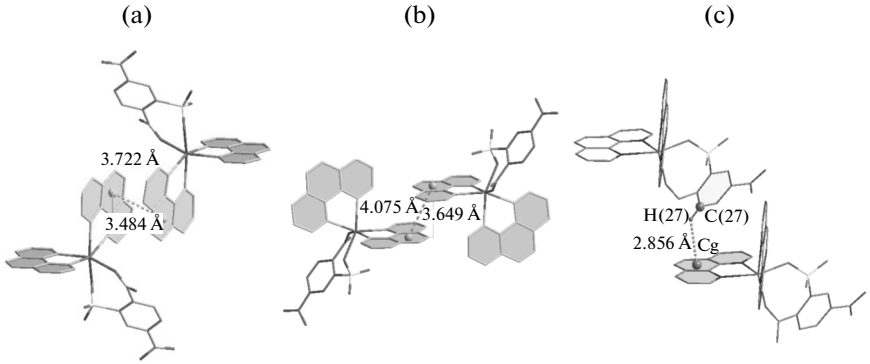

Fig. 4. The illustrations of π···π stacking interactions in **I**: the face-to-face mode between two *o*-Phen(1) molecules (a); the face-to-face mode between two *o*-Phen(2) molecules (b); the edge-to-face mode between C(27)–H(27)···Cg(1) (c).

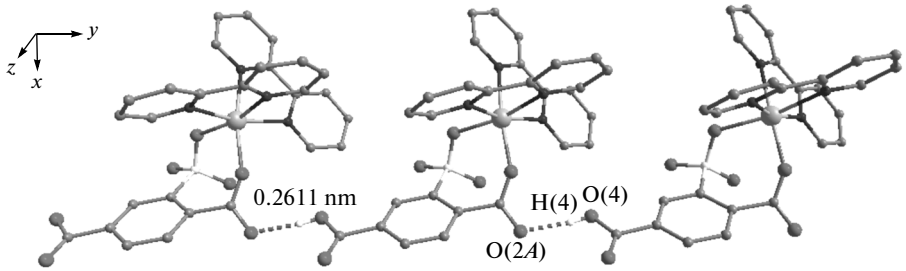

Fig. 5. 1D supramolecular chain based on H-bonds along *y* axis in **II**.

DMF solution (peak-to-peak separations ranging from −200...+600 mV at a rate of 200 mV s^{-1}). Both two complexes exhibit the quasi-reversible wave of single-electron, since the oxidation-reduction peaks are close to each other. The oxidation-reduction peaks at 0.184 (**I**) and 0.180 (**II**) V, 0.124 (**I**) and 0.123 (**II**) V corresponds to the conversion of Mn(III) and Mn(II) couples, which show that electron transfer between Mn(III) and Mn(II) in electrolysis is quasi-reversible process ($\Delta E_1 = 0.060$ V, $\Delta E_2 = 0.057$ V) [25–27]. This study is significant for extending the metal organic complexes containing electronic conjugated system.

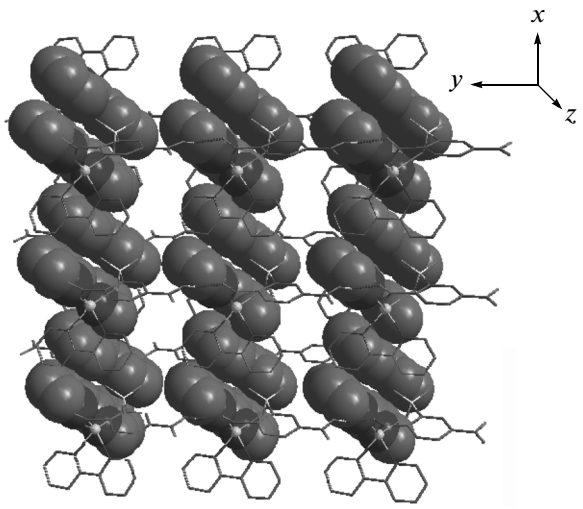

Fig. 6. 2D supramolecular layer in *xy* plane based on 2,2'-Bipy(1) in the face-to-face π···π interactions.

ACKNOWLEDGMENTS

This work was supported by the National Natural Science Foundation of China (no. 21003103), the Natural Scientific Research Foundation of Shaanxi Provincial Education Office of China (nos. 12JK0609 and 11JK0567).

REFERENCES

1. Weng, D.F., Wang, Z.M., and Gao, S., *Chem. Soc. Rev.*, 2011, vol. 40, p. 3157.
2. Xie, Z.G., Wang, C., de Krafft, K.E., and Lin, W.B., *J. Am. Chem. Soc.*, 2011, vol. 133, p. 2056.
3. Cheethan, A.K. and Rao, C.N.R., *Science*, 2007, vol. 318, p. 58.
4. Zhang, M.B., Chen, H.M., Hu, R.X., and Chen, Z.L., *CrystEngComm*, 2011, vol. 13, p. 7019.
5. Liu, D., Ren, Z.G., Li, H.X., et al., *CrystEngComm*, 2010, vol. 12, p. 1912.
6. Zheng, S.T., Wu, T., Zhang, J., et al., *Angew. Chem. Int. Ed.*, 2010, vol. 49, p. 5362.
7. Chen, M.S., Tan, X.W., Zhang, C.H., and Kuang, D.Z., *Z. Anorg. Allg. Chem.*, 2011, vol. 637, p. 1220.
8. Zhang, M.L., Xing, F.G., and Wang, Z.L., *Chin. J. Struct. Chem.*, 2010, vol. 29, p. 592.
9. Ren, P., Shi, W., and Cheng, P., *Cryst. Growth Des.*, 2008, vol. 8, p. 1097.
10. Taguchi, T., Wernsdorfe, W., Abboud, K.A., and Christou, G., *Inorg. Chem.*, 2010, vol. 49, p. 10579.
11. Meng, M., Zhong, D.C., and Lu, T.B., *CrystEngComm*, 2011, vol. 13, p. 6794.
12. Xiao, H.P., Zheng, Y.X., Liang, X.Q., et al., *J. Mol. Struct.*, 2008, vol. 888, p. 55.
13. Horike S., Matsuda R., Tanaka D., et al., *Angew. Chem. Int. Ed.*, 2006, vol. 45, p. 7226.
14. Lian, Z.X., Zhang, J.M., Xu, M.L., et al., *Acta Crystallogr. C*, 2007, vol. 63, p. m445.
15. Horike, S., Matsuda, R., Tanaka, D., et al., *J. Am. Chem. Soc.*, 2006, vol. 128, p. 4222.
16. Horike, S., Bureekaew, S., and Kitagawa, S., *Chem. Commun.*, 2008, p. 471.
17. Siemens, *SAINT*, *Area Detector Control and Iintegration Software*, Madison (WI, USA): Siemens Analytical X-ray Instruments Inc., 1996.
18. Sheldrick, G.M., *SHELX-97 and SHELXTL*, *Software Reference Manual*, *Version 5.1*, Madison (WI, USA): Brucker AXS Inc., 1997.
19. Sheldrick, G.M., *SADABS*, *Program for Empirical Absorption Correction of Area Detector Data*, Göttingen (Germany): Univ. of Göttingen, 1996.
20. Wen, L.L., Wang, F., Feng, J., et al., *Cryst. Growth Des.*, 2009, vol. 9, p. 3581.
21. Forbes T.Z. and Sevov S.C., *Inorg. Chem.*, 2009, vol. 48, p. 6873.
22. Liu C.M., Zhang D.Q., and Zhu, D.B., *Inorg. Chem.*, 2009, vol. 48, p. 792.
23. Wang, J., Zheng, S.L., Hu, S., et al., *Inorg. Chem.*, 2007, vol. 46, p. 795.
24. Fan, R.Q., Wang, P., Ren, J.Y., et al., *Spectroscopy and Spectral Analysis*, 2011, vol. 31, p. 1734.
25. Ding, Y., Xia, C.F., Hu, Z.Q., et al., *Acta Chim. Sinica*, 2009, vol. 14, p. 1579.
26. Lv, Y.K., Feng, Y.L., Liu, J.W., et al., *Chin. J. Inorg. Chem.*, 2011, vol. 27, p. 791.
27. Yan, S.H., Jiang, D.M., Zhang, Y., et al., *Chin. J. Inorg. Chem.*, 2011, vol. 27, p. 1191.